CellFIE: CRISPR- and cell fusion-based two-hybrid interaction mapping of endogenous proteins

Secker C., Kostova S., Niederlechner H., Beetz S., Wendland I., Liebich M.J., Polzer O., Groh M., Schnoegl S., Trepte P., Wanker E.E.

This is the final version of the accepted manuscript. The original article has been published in final edited form in:

Journal of Molecular Biology
2021 DEC 03 ; 433(24):167305
2021 OCT 14 (first published online: final publication)
doi: 10.1016/j.jmb.2021.167305

Publisher: Elsevier

CellFIE: CRISPR- and c**ell f**usion-based two-hybrid **i**nteraction mapping of **e**ndogenous proteins

Christopher Secker[1,2,#], Simona Kostova[1,#], Hannah Niederlechner[1,2], Stephanie Beetz[1], Ina Wendland[1], Mara J. Liebich[1], Oliver Polzer[1], Mirjam Groh[1,2], Sigrid Schnoegl[1], Philipp Trepte[1,3,$,*] and Erich E. Wanker[1,$,*]

[1] Neuroproteomics, Max Delbrück Center for Molecular Medicine in the Helmholtz Association (MDC), Berlin, Germany

[2] Department of Neurology, Charité Universitätsmedizin Berlin, Berlin, Germany

[3] Brain Development and Disease, Institute of Molecular Biotechnology of the Austrian Academy of Sciences (IMBA), Vienna, Austria

[#,$] Contributed equally

[*] Corresponding authors: Erich Wanker (Tel: +49-30-9406-2157, E-mail: erich.w@mdc-berlin.de) and Philipp Trepte (Email: philipp.trepte@imba.oeaw.ac.at)

Abstract

Numerous genetic methods facilitate the detection of binary protein-protein interactions (PPIs) by exogenous overexpression, which can lead to false results. Here, we describe CellFIE, a CRISPR- and cell fusion-based PPI detection method, which enables the mapping of interactions between endogenously tagged two-hybrid proteins. We demonstrate the specificity and reproducibility of CellFIE in a matrix mapping approach, validating the interactions of VCP with ASPL and UBXD1, and the self-interaction of TDP-43 under endogenous conditions. Furthermore, we show that CellFIE can be used to quantify changes of endogenous PPIs upon stress induction or drug treatment. For the first time, CellFIE facilitates systematic mapping of interactions between endogenously tagged proteins and represents a novel tool to characterize PPIs in live cells under dynamic conditions.

Introduction

All processes in a cell rely on the dynamic assembly and disassembly of stable and transient multi-protein complexes[1]. Cellular protein networks are dominated by weak and transient interactions, whereas stable complexes represent the minority[2]. However, the interactome of a cell does not only depend on the binding affinity between proteins, but also on their concentration, localization and posttranslational modifications[3–5]. In the most widely used methods, protein-protein interactions (PPIs) are identified either by analysis of tagged proteins or by affinity purification of protein complexes using antibodies[6,7]. The former requires the exogenous overexpression of two-hybrid proteins, which can promote the assembly of non-physiological protein complexes or aggregates, have unwanted effects on cellular localization and homeostasis, and may lead to false-positive and -negative results[8]. The latter depends on the availability of specific antibodies, detects protein complex compositions rather than direct interactions[9] and requires cell lysis that often results in the loss of transient interactions[7]. Until today, only very few methods have been described that allow measuring the association of proteins expressed from their endogenous loci and in their native environment[10–12]. With the recent advances in genome engineering, genes can now be modified more easily at their genomic loci to generate knock-in cell lines endogenously expressing fluorescent or luminescent reporter proteins using the CRISPR/Cas9 system[13,14]. Continued improvements in genome editing will allow genome-scale knock-ins in the near future, which will enable the detection of binary interactions of endogenously tagged proteins and their quantification under different conditions. To perform systematic mapping of multiple proteins (e.g. of distinct pathways or complexomes), however, very large numbers of double knock-in cell lines endogenously expressing two tagged reporter proteins would need to be generated. Innovative approaches to make endogenous binary PPI mapping more efficient are

therefore required. Here, we describe CellFIE – a novel approach to perform CRISPR- and cell fusion-based interaction mapping of endogenously expressed two-hybrid proteins in live cells.

Results

To measure PPIs using CellFIE, the following procedure is applied: First, independent human haploid (eHAP[15]) donor and acceptor cell lines endogenously expressing NanoLuc luciferase (NL)- or mCitrine (mCit)-tagged proteins are generated by CRISPR/Cas9 genome editing[14]. Second, donor and acceptor cell lines are electrofused in order to endogenously express both NL- and mCit-tagged proteins in the same cell. Third, interactions are measured in fused cells by quantifying bioluminescence resonance energy transfer (BRET) between the NL and mCit tags (**Fig. 1a**). BRET occurs only if the proteins are in close proximity (<10 nm). Recently, the utility of BRET to detect both weak and strong interactions with high sensitivity and specificity has been demonstrated[16].

To validate the CellFIE approach, we selected four human proteins, namely VCP, ASPL, UBXD1 and TDP-43, for a focused proof-of-concept study. VCP is a AAA+ ATPase implicated in neurodegenerative diseases and cancer[17]. It has been previously shown to interact with the UBX domain proteins ASPL and UBXD1 in mammalian cells when exogenously expressed as NL- and mCit-tagged fusions[15]. TDP-43 is the main component of protein inclusions in amyotrophic lateral sclerosis (ALS) and frontotemporal lobar degeneration (FTLD); its dimerization was previously shown endogenously using antibody-based methods[16]. For PPI mapping with CellFIE, first donor or acceptor cell lines were generated by CRISPR-mediated knock-in of the NL gene at the loci of *ASPSCR1* (ASPL), *UBXN6* (UBXD1) and *TARDBP* (TDP-43) or the mCit gene at the loci of *VCP* and *TARDBP*, respectively. For PPI detection, haploid

donor and acceptor knock-in cell lines were subsequently fused (**Fig. 1b**). To enable double antibiotic selection of fused cells, genes encoding hygromycin or neomycin resistance were additionally integrated into the genome of haploid donor and acceptor cells, respectively. For C-terminal knock-ins, an internal ribosome entry site (IRES) followed by the hygromycin (donor cells) or neomycin (acceptor cells) resistance genes was inserted after the NL or the mCit tags, respectively (**Fig. 1c**). To allow double-antibiotic selection of fused cells with N-terminally tagged fusion proteins, we first generated recipient cell lines expressing either the hygromycin or the neomycin antibiotic-resistance gene constitutively from the adeno-associated virus integration site 1 (AAVS1) safe-harbor locus (**Fig. 1d**, left panel). With these recipient cell lines, we then performed knock-ins of NL or mCit after the first start codon of the selected target genes (**Fig. 1d,** right panel). An overview of the generated haploid CellFIE lines is shown in **Fig. 1e**. As controls, we additionally generated donor and acceptor cell lines that only express the NL or the mCit tag from the AAVS1 locus together with the respective resistance genes (AAVS1::T2A-HygroR-CAG-NL and AAVS1::T2A-NeoR-CAG-mCit, **Fig. 1e**).

For the generation of knock-in cell lines, guide RNA plasmids and homologous repair templates (HRTs) were designed, cloned and co-transfected into eHAP cells (**Supplementary Fig. S1a-h**). For each cell line, two independent single-cell clones were generated, genotyped by PCR (**Supplementary Fig. S2**), Sanger sequenced and validated by western blotting (**Supplementary Fig. S3a-i**). The independent clones show comparable expression levels of the tagged fusion proteins, but lower expression compared to the unmodified wild-type gene products (**Supplementary Fig. S3a-i**). However, between different knock-in clones we detected no significant difference in endogenous fusion construct expression (haploid lines, **Supplementary Fig. 3j,k**). In total, two recipient cell lines and 16 haploid eHAP cell lines (two individual

clones each) expressing control proteins from the AAVS1 locus or endogenously expressing NL- or mCit-tagged VCP, ASPL, UBXD1 and TDP-43 fusion proteins were produced (**Fig. 1e**/**Table 1**).

To systematically test binary interactions of endogenously expressed NL- and mCit-tagged hybrid proteins, we electrofused each haploid donor cell line with each haploid acceptor cell line (**Fig. 2a**). Four biologically independent fusion experiments were performed with two clones of each donor and acceptor cell line (**Supplementary Fig. S1i**). The fused cells were genotyped by PCR (**Supplementary Fig. S2a-k**); endogenous co-expression of fusion proteins was confirmed by western blotting (**Supplementary Fig. S3a-k**) and quantification of luminescence and fluorescence emission (**Supplementary Fig. S3l,m**). To evaluate whether CellFIE is able to specifically detect the binary interactions of ASPL and UBXD1 with VCP as well as the self-interaction of TDP-43 under endogenous conditions, we systematically assessed all generated CellFIE lines (8x8 matrix) for potential PPIs. To determine BRET ratios of the interaction pairs, luminescence was measured at short (370-480 nm, NL emission maximum) and long wavelengths (520-570 nm, mCit emission maximum through energy transfer); the donor control cell line expressing NL alone was used to correct for donor bleed-through (**Fig. 2b**). Strikingly, ASPL-NL lines fused with VCP-mCit and mCit-VCP lines showed significantly higher BRET ratios compared to ASPL-NL fused with mCit-TDP-43 or mCit-only lines (**Fig. 2b,c**). UBXD1-NL lines fused with mCit-VCP lines also showed significantly higher BRET ratios compared to UBXD1-NL lines fused with mCit-TDP-43 or mCit-only lines. Interestingly, fusion of UBXD1-NL lines with VCP-mCit lines did not result in elevated BRET ratios (**Fig. 2b,c**), confirming our published results from transient BRET experiments, in which the interaction between UBXD1 and VCP was also not detected with C-terminally tagged VCP[15]. With CellFIE, we were also able to validate the self-interaction between endogenous NL-

TDP-43 and mCit-TDP-43 (**Fig. 2b**), which showed a significantly higher BRET ratio compared to cell fusions between NL-TDP-43 lines with VCP-mCit, mCit-VCP or mCit only cell lines (**Fig. 2d**). Importantly, we detected no elevated BRET ratios for cell fusions of NL or mCit-only expressing lines with all other acceptor or donor cell lines, respectively, underlining the specificity of the method (**Fig. 2c,d**). In summary, we endogenously tested 16 binary PPIs in biological quadruplicates performing 64 cell fusions in total. Importantly, no false-positive interactions were detected, while we were able to detect all previously reported binary interactions at endogenous conditions (VCP/ASPL, VCP/UBXD1 and TDP-43/TDP-43).

Next, we investigated whether CellFIE can sensitively detect dynamic changes of endogenous PPIs under different conditions, such as stress and drug treatment. Therefore, we used the generated NL-TDP-43/mCit-TDP-43 and UBXD1-NL/mCit-VCP CellFIE lines and investigated TDP-43 dimer- and oligomerization as wells as the VCP/UBXD1 interaction under different conditions. TDP-43 is an RNA-binding protein, which is described to homo-oligomerize under physiological conditions via its N-terminus[18]. Under stress, however, TDP-43 is reported to undergo liquid-liquid phase separation (LLPS), which affects its self-interaction[19]. The AAA+ ATPase VCP was recently implicated in the disassembly of stress granules[20]. Interestingly, complex formation of VCP with UBX domain-containing proteins was observed after UV irradiation or $NaAsO_2$ treatment[21]. To first monitor the PPIs under stress, we treated CellFIE lines with 250 µM sodium arsenite ($NaAsO_2$) and analyzed the BRET interaction signals before and after 15, 60 and 180 min of treatment (**Fig. 3a**). Interestingly, NL-TDP-43/mCit-TDP-43 CellFIE lines showed a significant reduction of the BRET signal over time, indicating that the self-interaction of endogenous TDP-43 proteins is reduced (**Fig. 3b**). In contrast, treatment of UBXD1-NL/mCit-VCP CellFIE lines with $NaAsO_2$ leads to a temporary increase of the endogenous interaction signal

after 60 min, which quickly recovered to interaction level of untreated cells after 180 min (**Fig. 3c**). This demonstrates that CellFIE is able to sensitively detect dynamic changes of PPIs over time in live cells.

Additionally, we investigated whether CellFIE can detect drug effects on endogenous PPIs. Therefore, we treated NL-TDP-43/mCit-TDP-43 and UBXD1-NL/mCit-VCP CellFIE lines with different concentrations of the VCP AAA+ ATPase inhibitors CB-5083 and NMS-873. These compounds were developed for cancer therapy and are reported to inhibit the ATPase activity of VCP in *in vitro* experiments with a half maximal inhibitory concentration (IC_{50}) of 11 nM and 30 nM, respectively[22,23]. To investigate whether the compounds modulate the interaction between VCP and its interaction partner UBXD1, we treated the CellFIE lines with increasing compound concentrations from 0.1 nM to 10 µM for 180 min and quantified interactions by BRET (**Fig. 3d**). As a control, we applied the same compounds to NL-TDP-43/mCit-TDP-43 CellFIE lines (**Fig. 3e,f**) and additionally treated UBXD1-NL/mCit-VCP and NL-TDP-43/mCit-TDP-43 CellFIE lines with the well-characterized BCL protein family PPI inhibitor Navitoclax (ABT-263, **Fig. 3g**). Interestingly, we observed a strong concentration-dependent reduction of the endogenous UBXD1-NL/mCit-VCP interaction signals after treatment with the ATPase inhibitors CB-5083 and NMS-873, respectively (red data points, **Fig. 3e,f**). Treatment of NL-TDP-43/mCit-TDP-43 CellFIE lines also lead to a moderate reduction in BRET signal, however, only at higher concentrations (blue data points, **Fig. 3e,f**). While the IC_{50} values of CB-5083 and NMS-873 for the UBXD1-NL/mCit-VCP interaction was 75 and 432 nM, respectively, it was ~8- (579 nM) and ~9-fold (3.9 µM) higher for the endogenous NL-TDP-43/mCit-TDP43 interaction, respectively. This indicates that the two ATPase inhibitors both potently influence the interaction between VCP and UBXD1. Notably, the treatment of both CellFIE lines with the BCL PPI inhibitor

ABT-263[24] did not result in a reduction of the interaction signals, respectively (**Fig. 3g**). Thus, CellFIE is able to sensitively detect drug effects on PPIs in mammalian cells.

Discussion

CellFIE combines CRISPR genome engineering, mammalian cell fusion and BRET quantification, enabling for the first-time systematic testing of binary interactions between endogenously tagged proteins in live cells. To study binary interactions endogenously without cell fusion, reporter-tags would need to be introduced at the two genomic loci of interest for each protein pair to be tested within the same cell line. For systematic PPI mapping, this would require the generation of a large amount of double knock-in cell lines. In concrete figures this means that, when mapping 10x10 PPIs, a double knock-in approach would require the generation of 100 genetically modified cell lines. Using CellFIE, each haploid donor knock-in cell line can be fused with any other acceptor line and the investigation of 10x10 protein pairs only requires the generation of 20 cell lines. While the number of knock-in lines to be generated increases exponentially for a double knock-in strategy, it only increases linearly for the CellFIE approach (x^2 vs. $x*2$, where x=number of unique proteins to be mapped). Due to the relatively laborious step to generate endogenously tagged cell lines, the fusion approach is therefore numerically much more efficient when performing endogenous PPI mapping at higher scale. The approach to first generate haploid knock-in cells and subsequently fuse them to a compatible counterpart could also be extended to other tag-based readouts.

While the generated haploid knock-in lines are homozygous, fused CellFIE lines always contain one tagged and one untagged allele of both loci of interest. We found that the endogenous tagging of genes with NL or mCit can result in reduced protein expression (**Supplementary Fig. 3**). It can be argued that when non-tagged proteins

are expressed at higher levels, this could negatively affect sensitivity since only tagged proteins contribute to the PPI signal. While this has not been an issue for the limited number of interactions quantified in this study, it cannot be excluded that decreased expression after endogenous tagging prevents final PPI detection for individual protein pairs. However, our published data show that NL-based BRET assays are very sensitive and PPIs can be detected even when transient expression of reporter proteins is below the levels of endogenously expressed, untagged proteins[16].

Since CellFIE uses a specific haploid cell line[15] for endogenous PPI testing, it is *per se* limited to the investigation of interacting proteins that are natively expressed in eHAP cells. To assess the endogenous abundance of target proteins in eHAP cells, we have analyzed a publicly available RNAseq dataset[25]. Our investigation indicates that 70-80% of all human protein-encoding genes are expressed in eHAP cells (>0.5-1.0 transcripts per kilobase million (TPM), **Supplementary Table 1**). Importantly, our proof-of-concept study demonstrates that interactions between proteins expressed at relatively high (*VCP*, 46.50 TPM; *TARDBP*, 33.15 TPM) as well as at relatively low levels (*ASPSCR1*, 3.44 TPM; *UBXN6*, 5.10 TPM) can be detected with CellFIE. Potential strategies to measure interactions between proteins with CellFIE, which are not natively expressed in eHAP cells (<0.5 TPM, **Supplementary Table 1**), could include the activation of gene expression by CRISPR/Cas[26] and other engineered transcription factors[27,28], or the transcription factor-mediated, direct differentiation of eHAP cells into other cell types[29].

Recently, it was shown that the endogenous expression of reporter proteins enables the real time analysis of biological processes that cannot be observed using overexpression-based approaches[30]. To assess the potential of CellFIE to quantify changes of PPIs under such dynamic conditions, we have analyzed CellFIE lines upon stress induction or drug treatment. While we have previously shown that drug effects

and heat shock-induced PPI changes can also be investigated in cells overexpressing BRET fusion proteins[16], exogenous overexpression was shown to affect PPI dynamics[31]. Thus, cellular PPIs should be captured more accurately and with less potential for artifacts[8] when using endogenously expressed PPI reporters such as CellFIE. Indeed, we found that CellFIE sensitively detects changes of endogenous PPIs upon stress induction over time and can be used to determine half maximal inhibitory drug concentrations for endogenously interacting proteins in live cells. Apart from stress induction or drug treatment, additional conditions such as starvation, viral or bacterial infection, exposure to toxins or introduction of disease-mutations, could inform us of whether specific PPIs are involved in or are affected by such processes. Additionally, quantifying endogenous PPIs upon drug treatment could support the preclinical identification of undesirable, off-target drug effects, e.g. the stabilization of oncogenic or the destabilization of tumor suppressing PPIs. Further, it could help assessing the efficacy and specificity of PPI modulating drugs under native expression conditions. In summary, we suggest that CellFIE is highly useful to systematically map and validate protein complexes under endogenous conditions and to study their modulation by drugs or regulation under various cellular conditions.

Methods

Design and cloning of HRT and gRNA plasmids

Selection and evaluation of gRNAs for the *ASPSCR1* (ASPL), *UBXN6* (UBXD1), *VCP* (VCP) and *TARDBP* (TDP-43) loci of interest as well as the selection of ~800 bp long sequences for the 5’ and 3’ homology arms for the HRTs were performed with Benchling (https://www.benchling.com/). The gRNA sequence for the AAVS1 locus was described before[19]. A Cas9 expressing plasmid containing a puromycin resistance (pSpCas9(BB)-2A-Puro (PX459) V2.0) was a gift from Feng Zhang (Addgene #62988).

It was used to insert the preformed gRNA oligo duplex containing the respective guide sequences (Table 2) via Golden Gate Assembly according to the protocol published[20]. HRTs for ASPL-NL IRES-Hygro, mCit-VCP and VCP-mCit IRES-Neo were gene synthesized and subcloned into the pMK cloning vector by GeneArt™ (ThermoFisher). HRTs for UBXD1-NL IRES Hygro, NL- and mCit-TDP-43 were cloned. In brief, homology arms ~800 bp upstream and downstream of the gRNA targets were PCR amplified from genomic DNA of wild-type eHAP cells (primers are listed in Table 2). NL (IRES-Hygro) and mCit inserts as well as the pMK vector backbone were PCR amplified from synthesized ASPL- and VCP-HRTs. Finally, all PCR fragments were joined using Gibson assembly. HRT plasmid pAAVS1-Hygro-CAG-DEST was generated from pAAVS1-Nst-CAG-DEST (Addgene #80489 plasmid was a gift from Knut Woltjen). The neomycin resistance gene was removed from pAAVS1-Nst-CAG-DEST by restriction digestion with SpeI and SacI, then the hygromycin resistance gene was PCR amplified from Hygro-iDEST with primers #19 and #20 (Addgene #75339 plasmid was a gift from Danwei Huangfu) and resulting fragments were joined using Gibson assembly. For generating the recipient cell line HRTs AAVS1-Nst and AAVS1-Hygro, the Gateway cassette was removed from pAAVS1-Nst-CAG-DEST and pAAVS-Hygro-CAG-DEST by PCR amplification using 5’-phosphorylated primers #21 and #22 or #23 and #24, respectively, and subsequent ligation. For the NL and mCit control cell lines, HRTs targeting the AAVS1 locus were produced. Therefore, we first generated entry vectors by PCR amplifying the sequences of interest. Resulting fragments were shuttled into pDONR221 (Invitrogen) using the BP clonase (Invitrogen). The cDNA encoding the NL was amplified using primers #44 and #45 from vector pNL1.1 (Promega). The cDNA encoding mCit was amplified using primers #46 and #47 from vector pcDNA3.1 PA-mCit[15]. The resulting NL and mCit entry vectors were shuttled into the HRT destination vectors pAAVS1-Hygro-CAG-DEST and

pAAVS1-Neo-CAG-DEST using the LR clonase technology according to the manufacturer's instructions (Invitrogen). All gRNA sequences and primers are listed in Table 2.

Cell culture and transfection

The human eHAP cell line (Horizon Discovery, C669) was cultured at 37°C and 5% CO_2 in IMDM medium (Gibco™, Thermo Fisher) supplemented with 10% heat inactivated fetal bovine serum (FBS; Gibco™, Thermo Fisher) and 1% penicillin/streptomycin (Gibco™, Thermo Fisher). Cells were passaged every 2-3 days by splitting approximately 1:10-1:20 using 0.05% Trypsin-EDTA (Gibco™ ThermoFisher). For knock-in generation $1x10^6$ haploid eHAP cells were transfected with 1 µg of HRT and 1 µg of the respective gRNA plasmid using the FuGENE® HD transfection reagent (Promega) following the manufacturer´s instructions.

Selection and single clone isolation

Cells were selected for 72 hours by adding puromycin (0.5 µg/ml) to the cell culture medium 8-24 hours after transfection. Knock-ins were selected by hygromycin (1 mg/ml) or geneticin (G418; 4 mg/ml) addition, or by fluorescence activated cell sorting on a BD Biosciences FACS Aria I, II or III. From the remaining cell pool, single-cell clones were grown, by seeding one cell in every third well of a 96-well plate. Cultivation was continued until visible colonies appeared. Single clones were further characterized and validated by western-blotting, PCR genotyping and Sanger sequencing.

Genotyping and western blotting

Genomic DNA samples of knock-in and fused cell lines were prepared with QuickExtract™ DNA Extraction Solution (Lucigen®) or DNeasy® Blood and Tissue kit

(Qiagen) according to the manufacturer's manual. For the genotyping PCR, 2.5 µl or 100 ng genomic DNA were used in a 25 µl PCR reaction, using the Phusion Hot Start DNA Polymerase with GC buffer (NEB) and 5% DMSO supplement. All resulting PCR products were analyzed on a 0.8% TAE agarose gel and clones with correct amplicon sizes were subjected to Sanger sequencing. Sequences of the primers used for genotyping are listed in Table 2.

Samples for western blot analysis were prepared by lysing cells in a standard HEPES-buffer (50 mM, pH 7.4, 150 mM NaCl) containing 1% of NP-40, 0.5% deoxycholate, 10% glycerol, 20 mM NaF, 1.5 mM $MgCl_2$, 1 mM EDTA, 1 mM PMSF, 1U Benzonase and a protease inhibitor cocktail (Roche, EDTA-free). The total protein concentration was determined by a BCA assay (Pierce™) and equal amounts of protein were loaded on a NuPAGE™ Novex™ 4-12% Bis-Tris precast polyacrylamide gel (Thermo Fisher). Running conditions were adjusted to 80 min and 120 V. The proteins were blotted on a nitrocellulose membrane (0.45 µM, Amersham™ Protran) with the wet blot system by BioRad for 60 min at 100 V. The primary antibodies were as follows: anti-TUG (rabbit monoclonal, Abcam, ab131217, 1:3000), anti-VCP (mouse monoclonal, Progen, 65278, 1:5000), anti-α-Tubulin (mouse monoclonal, Sigma-Aldrich, T6074, 1:2000), anti-UBXN6 (mouse monoclonal, Abcam, ab80659, 1:5000), anti-TDP-43 (rabbit polyclonal, ProteinTech, 10782-2-AP, 1:2000) and anti-Histone-H3 (rabbit polyclonal, Abcam, ab1791, 1:2000).

Cell fusion

Individual clones of validated donor and acceptor cell lines were each resuspended in a hypoosmolar electrofusion buffer (90 mOsmol/kg, Eppendorf, 4308 070.528) and respectively mixed in a 1:1 ratio (1.5 or 3.0 x 10^6 cells of each line) in a helix chamber of the Eppendorf Multiporator device. Electrofusion was performed as described by the

manufacturer: cells were first aligned by a 5 V pulse for 30 or 60 s, followed by one or two 27 V fusion pulses for 15 µs before cells were post-aligned at 5 V for 30 s. Fused cells were recovered overnight and subsequently selected by a double antibiotic treatment with hygromycin (1 mg/ml) and geneticin (4 mg/ml) starting 24 hours after fusion. During the selection process antibiotics concentrations were reduced to 0.6 mg/ml (hygromycin) and 2 mg/ml (geneticin) once the negative control (non-fused, co-cultivated cells) was less than 30% confluent. The antibiotics selection was prolonged until no surviving cells were detected in the non-fused negative control.

BRET measurements

All fused cell lines and the control cell line expressing only NL were seeded on white 96-well plates (Greiner bio-one: 655983) 24 hours before measurements. Each cell line was seeded in phenol red free IMDM media (Gibco, 21056023) supplemented with 10% FBS (Gibco™, Thermo Fisher) and 1% penicillin/streptomycin (Gibco™, Thermo Fisher) in three wells on two identical 96-well plates, resulting in six technical replicates per cell line. After measuring mCit fluorescence (ex. 500 nm/em. 530 nm), Coelenterazine-h (Promega S2011, PJK 102182) was added to each well of the 96-well plate at a final concentration of 5 µM. After 15 min of incubation at 37°C, total luminescence and luminescence at long (520-570 nm) and short (370-480 nm) wavelengths was quantified in a TECAN M1000Pro plate reader. BRET ratios were calculated as described previously[15]. For each experiment, background fluorescence and luminescence was obtained from eHAP wild-type cells and values were subtracted from obtained intensities of knock-in cells.

PPI detection under stress and drug treatment

For stress induction, fused eHAP cells (CellFIE lines) co-expressing NL-TDP-43 and mCit-NL-TDP-43 were seeded in a 96-well microtiter plate (8.250 cells per well) and were treated 48 hours later with 250 µM sodium arsenite ($NaAsO_2$) (S7400, Sigma-Aldrich) for 0, 15, 60 and 180 min, respectively. BRET measurements were performed at each designated time point as described above. Cells not treated with $NaAsO_2$ were also subjected to BRET measurements at the same time points (non-treated control) and all data points were normalized to the BRET signal at 0 min (nBRET). For drug treatment, CellFIE lines co-expressing UBXD1-NL and mCit-VCP were seeded in a 96-well microtiter plate (50.000 cells per well). 24 hours later, cells were treated in triplicates with 0.001, 0.01, 0.1, 1, 5 and 10 µM of VCP AAA+ ATPase inhibitor CB-5083 (Selleckchem) or DMSO as control for 180 min and BRET measurements were performed as described above.

Acknowledgments

This work was supported by grants from the German Research Foundation (SFB740:740/2-11), the Federal Ministry of Education and Research (Integrament: 01ZX1314C, ERA-NET NEURON: 01W1301), the European Union (EuroSpin: Health-F2-2009-241498 and SynSys: HEALTH-F2-2009-242167) and the Helmholtz Initiative on Personalized Medicine (iMED) to EEW, the CHDI foundation, the German Cancer Consortium DKTK (Germany) and the Deutsche Krebshilfe, ENABLE (Germany) to EEW and PT, as well as by the ALS Fellowship of the Charité to CS managed by the Stifterverband für die Deutsche Wissenschaft and founded by the Dr. Martin Herrenknecht Verwaltungs GmbH. The funders had no role in the study design, the collection and analysis of data or the preparation of the manuscript. We thank the Flow Cytometry technology platform of the Max Delbrück Center, where cell sorting was performed.

Author Contributions

PT and EEW conceived the study. PT, CS, SK and EEW designed the method, planned the experiments and analyzed the data. CS, PT and SK designed gRNAs and HRTs, and CS, SK, PT, HN and IW cloned all plasmids. CS, SK, PT, HN, SB, IW, MJL, OP and MG generated the knock-in cell lines, performed the PCR genotyping, western-blotting, cell fusions and BRET measurements. All authors discussed the results and CS, PT, EEW, SK and SS wrote the manuscript with comments from all authors.

Conflict of interest

The authors declare that they have no conflict of interest.

References

1. Perkins, J. R., Diboun, I., Dessailly, B. H., Lees, J. G. & Orengo, C. Transient protein-protein interactions: structural, functional, and network properties. *Structure* **18**, 1233–1243 (2010).

2. Hein, M. Y. *et al.* A human interactome in three quantitative dimensions organized by stoichiometries and abundances. *Cell* **163**, 712–723 (2015).

3. Larance, M. & Lamond, A. I. Multidimensional proteomics for cell biology. *Nat Rev Mol Cell Biol* **16**, 269–280 (2015).

4. Buntru, A., Trepte, P., Klockmeier, K., Schnoegl, S. & Wanker, E. E. Current Approaches Toward Quantitative Mapping of the Interactome. *Front Genet* **7**, 74 (2016).

5. Cafarelli, T. M. *et al.* Mapping, modeling, and characterization of protein-protein interactions on a proteomic scale. *Curr Opin Struct Biol* **44**, 201–210 (2017).

6. Snider, J. *et al.* Fundamentals of protein interaction network mapping. *Mol Syst Biol* **11**, 848 (2015).

7. Meyer, K. & Selbach, M. Quantitative affinity purification mass spectrometry: a versatile technology to study protein-protein interactions. *Front Genet* **6**, 237 (2015).

8. Gibson, T. J., Seiler, M. & Veitia, R. A. The transience of transient overexpression. *Nat Methods* **10**, 715–721 (2013).

9. Huttlin, E. L. *et al.* Dual proteome-scale networks reveal cell-specific remodeling of the human interactome. *Cell* **184**, 3022-3040.e28 (2021).

10. Komatsubara, A. T., Goto, Y., Kondo, Y., Matsuda, M. & Aoki, K. Single-cell quantification of the concentrations and dissociation constants of endogenous proteins. *J Biol Chem* **294**, 6062–6072 (2019).

11. Sadaie, W., Harada, Y., Matsuda, M. & Aoki, K. Quantitative in vivo fluorescence cross-correlation analyses highlight the importance of competitive effects in the regulation of protein-protein interactions. *Mol Cell Biol* **34**, 3272–3290 (2014).

12. Söderberg, O. *et al.* Direct observation of individual endogenous protein complexes in situ by proximity ligation. *Nat Methods* **3**, 995–1000 (2006).

13. Fueller, J. *et al.* CRISPR-Cas12a-assisted PCR tagging of mammalian genes. *J Cell Biol* **219**, (2020).

14. Koch, B. *et al.* Generation and validation of homozygous fluorescent knock-in cells using CRISPR-Cas9 genome editing. *Nat Protoc* **13**, 1465–1487 (2018).

15. Essletzbichler, P. *et al.* Megabase-scale deletion using CRISPR/Cas9 to generate a fully haploid human cell line. *Genome Res* **24**, 2059–2065 (2014).

16. Trepte, P. *et al.* LuTHy: a double-readout bioluminescence-based two-hybrid technology for quantitative mapping of protein-protein interactions in mammalian cells. *Mol Syst Biol* **14**, e8071 (2018).

17. Meyer, H., Bug, M. & Bremer, S. Emerging functions of the VCP/p97 AAA-ATPase in the ubiquitin system. *Nature Cell Biology* **14**, 117–123 (2012).

18. Afroz, T. *et al.* Functional and dynamic polymerization of the ALS-linked protein TDP-43 antagonizes its pathologic aggregation. *Nat Commun* **8**, 45 (2017).

19. Wang, A. *et al.* A single N-terminal phosphomimic disrupts TDP-43 polymerization, phase separation, and RNA splicing. *EMBO J* **37**, (2018).

20. Gwon, Y. *et al.* Ubiquitination of G3BP1 mediates stress granule disassembly in a context-specific manner. *Science* **372**, eabf6548 (2021).

21. Hülsmann, J. *et al.* AP-SWATH Reveals Direct Involvement of VCP/p97 in Integrated Stress Response Signaling Through Facilitating CReP/PPP1R15B Degradation*. *Molecular & Cellular Proteomics* **17**, 1295–1307 (2018).

22. Anderson, D. J. *et al.* Targeting the AAA ATPase p97 as an Approach to Treat Cancer through Disruption of Protein Homeostasis. *Cancer Cell* **28**, 653–665 (2015).

23. Magnaghi, P. *et al.* Covalent and allosteric inhibitors of the ATPase VCP/p97 induce cancer cell death. *Nat Chem Biol* **9**, 548–556 (2013).

24. Lock, R. *et al.* Initial testing (stage 1) of the BH3 mimetic ABT-263 by the pediatric preclinical testing program. *Pediatric Blood & Cancer* **50**, 1181–1189 (2008).

25. Casey S. Greene, Dongbo Hu, Richard W. W. Jones, Stephanie Liu, David S. Mejia, Rob Patro, Stephen R. Piccolo, Ariel Rodriguez Romero, Hirak Sarkar, Candace L. Savonen, Jaclyn N. Taroni, William E. Vauclain, Deepashree Venkatesh Prasad, Kurt G. Wheeler. refine.bio: a resource of uniformly processed publicly available gene expression datasets. *Refine.bio SRP044391, provided by Nijman Lab* https://www.refine.bio/experiments/SRP044391/.

26. Perez-Pinera, P. *et al.* RNA-guided gene activation by CRISPR-Cas9-based transcription factors. *Nat Methods* **10**, 973–976 (2013).

27. Zhang, F. *et al.* Efficient construction of sequence-specific TAL effectors for modulating mammalian transcription. *Nat Biotechnol* **29**, 149–153 (2011).

28. Beerli, R. R. & Barbas, C. F. Engineering polydactyl zinc-finger transcription factors. *Nat Biotechnol* **20**, 135–141 (2002).

29. Fernandopulle, M. S. *et al.* Transcription Factor-Mediated Differentiation of Human iPSCs into Neurons. *Curr Protoc Cell Biol* **79**, e51 (2018).

30. Schwinn, M. K., Steffen, L. S., Zimmerman, K., Wood, K. V. & Machleidt, T. A Simple and Scalable Strategy for Analysis of Endogenous Protein Dynamics. *Sci Rep* **10**, 8953 (2020).

31. White, C. W., Caspar, B., Vanyai, H. K., Pfleger, K. D. G. & Hill, S. J. CRISPR-Mediated Protein Tagging with Nanoluciferase to Investigate Native Chemokine Receptor Function and Conformational Changes. *Cell Chemical Biology* **27**, 499-510.e7 (2020).

Figures and Figure legends

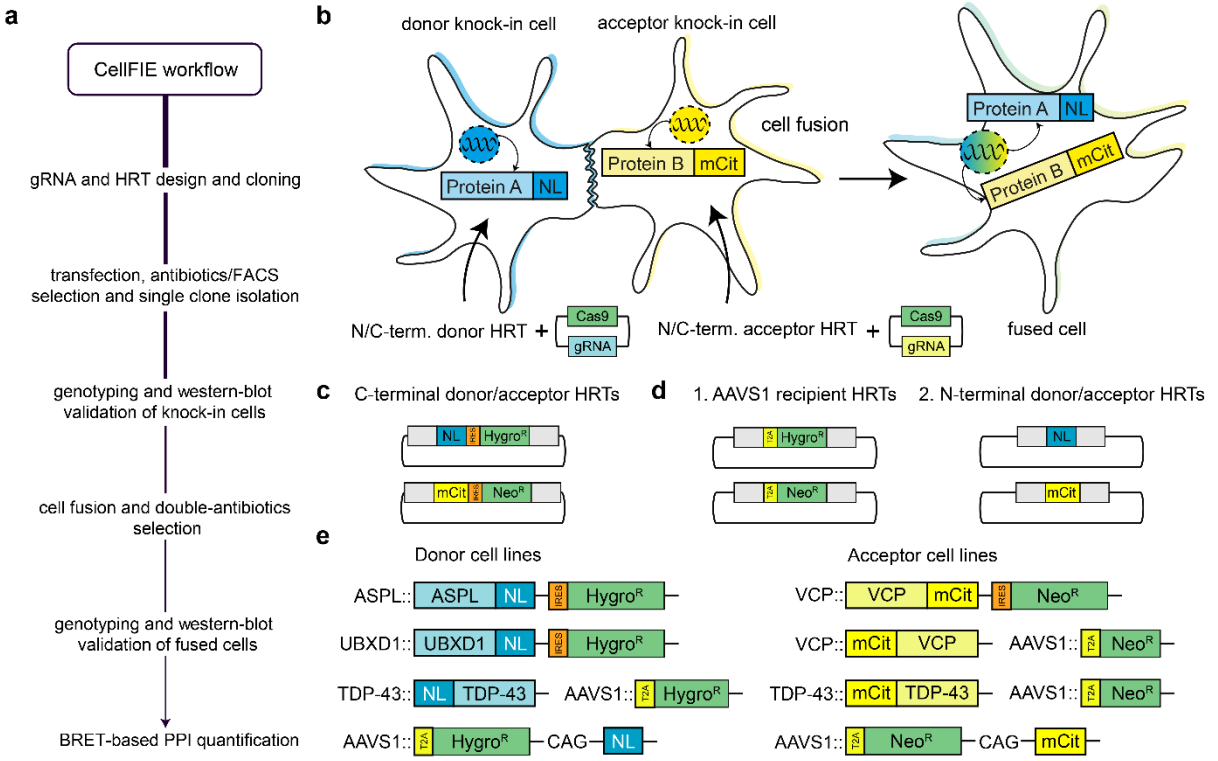

Fig. 1. The CellFIE procedure. (**a**) Stepwise overview of the workflow to detect interactions by CellFIE. (**b**) Schematic representation of the CellFIE method. Independent donor and acceptor cell lines are generated by co-transfecting Cas9 and gRNA plasmids together with homologous repair templates (HRT) to express NL- and mCit-tagged proteins from their endogenous loci. After cell fusion, the tagged proteins are endogenously expressed in the same cell. (**c**) For C-terminal donor or acceptor knock-ins, HRTs with the NL gene followed by an IRES site and a hygromycin resistance or the mCit gene followed by an IRES site and a neomycin resistance, respectively, are used. (**d**) For N-terminal donor or acceptor knock-ins, first recipient cell lines expressing a hygro- or neomycin resistance from the AAVS1 locus, respectively, were generated. Then, N-terminal acceptor or donor lines were generated by knocking in the NL or mCit gene into the respective hygro- or neomycin resistant recipient cell lines. (**e**) Schematic representation of genomic loci of cell lines generated to investigate the interactions between ASPL-NL, UBXD1-NL, NL-TDP-43 and mCit-

VCP, VCP-mCit or mCit-TDP-43 in proof-of-principle CellFIE experiments. Control cell lines only express NL and the hygromycin resistance or mCit and the neomycin resistance, respectively, from the AAVS1 safe harbor locus.

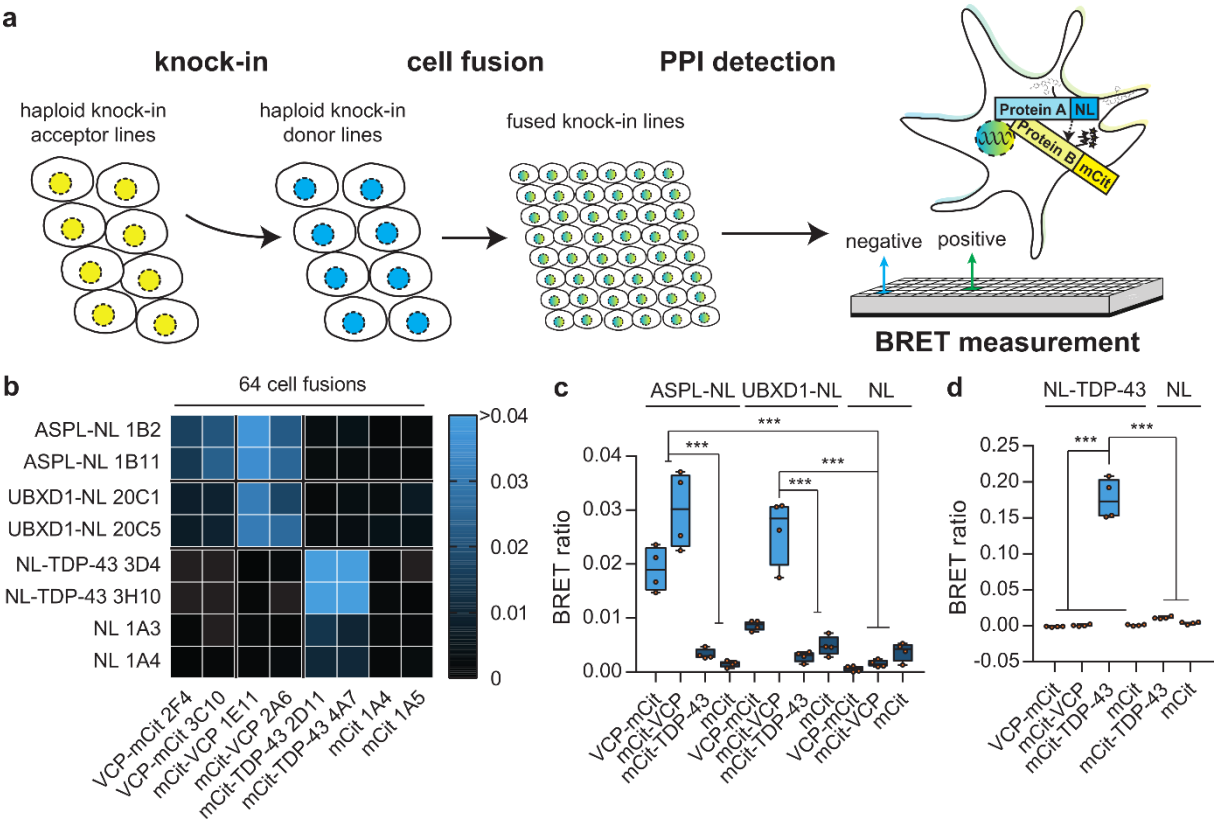

Fig. 2. Endogenous interaction mapping using CellFIE. (**a**) Schematic overview of the interaction mapping procedure; eight acceptor and eight donor cell lines (n=64 fused lines) were electrofused. (**b**) Heat-map showing the mean BRET ratios (n=6) of each CellFIE line. (**c,d**) Box and whiskers showing minimum to maximum and mean of all four data points of ASPL-NL, UBXD1-NL or NL (**c**) and NL-TDP-43 or NL (**d**) fused to all acceptor lines. Four independent fusions were performed per interaction (n=4). Significance was calculated by one-way ANOVA followed by Sidak multiple comparisons *post hoc* test; *** p<0.001.

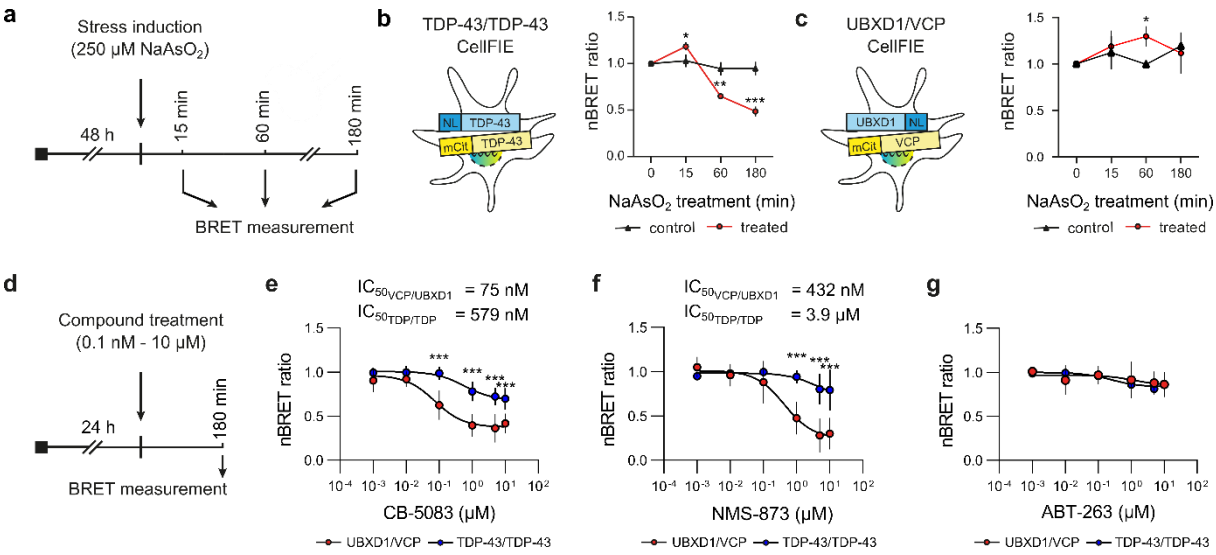

Fig. 3. Quantification of PPIs with CellFIE under stress and drug treatment. (**a**) Scheme of stress induction experiment. Endogenous NL-TDP-43/mCit-TDP-43 (**b**) and UBXD1-NL/mCit-VCP (**c**) CellFIE lines were treated with 250 µM $NaAsO_2$ and interactions were quantified by measuring BRET after 15, 60 and 180 min. (**b,c**) Plots show normalized BRET (nBRET) values of $NaAsO_2$ treated (red lines) and untreated (black lines) CellFIE lines over time. BRET ratios were normalized to signal before treatment (0 min). Data points represent mean of three biological replicates ± SD, *n* = 3. $NaAsO_2$ treated samples were compared to untreated controls by paired student's t-test, * p<0.05, ** p<0.01, *** p<0.001. (**d**) Scheme of compound treatment experiments. Cells were treated with 0.001, 0.01, 0.1, 1, 5 and 10 µM of VCP-binding compounds CB-5083 (**e**) and NMS-873 (**f**) or BCL PPI inhibitor Navitoclax (ABT-263) (**g**) as control. Endogenous UBXD1-NL/mCit-VCP (red data points) and NL-TDP-43/mCit-TDP-43 interaction signals (blue data points) were quantified by measuring BRET after 180 min. BRET ratios were normalized to solvent (DMSO) control. Data points represent mean ± SD from four to six individual experiments and two individual fusions each. Data points were non-linearly fitted to calculate IC_{50}. The effect of each compound concentration on the UBXD1-NL/mCit-VCP interaction was compared to

the response on the NL-TDP-43/mCit-TDP-43 interaction by two-way ANOVA and Sidak multiple comparison test, *** $p<0.001$.

Table 1: Overview of haploid knock-in cell lines generated.

#	Name	Type	Parental cell line	Application
	ASPL:			
1	ASPL-NL-IRES-Hygro 1B2	donor cell line	eHAP wild-type	PPI mapping
2	ASPL-NL-IRES-Hygro 1B11	donor cell line	eHAP wild-type	PPI mapping
	UBXD1:			
3	UBXD1-NL-IRES-Hygro 20C1	donor cell line	eHAP wild-type	PPI mapping
4	UBXD1-NL-IRES-Hygro 20C5	donor cell line	eHAP wild-type	PPI mapping
	VCP:			
5	VCP-mCit-IRES-Neo 2F4	acceptor cell line	eHAP wild-type	PPI mapping
6	VCP-mCit-IRES-Neo 3C10	acceptor cell line	eHAP wild-type	PPI mapping
7	mCit-VCP 1E11	acceptor cell line	AAVS1::Neo	PPI mapping
8	mCit-VCP 2A6	acceptor cell line	AAVS1::T2A-Neo	PPI mapping
	TDP-43:			
9	NL-TDP-43 3D4	donor cell line	AAVS1::T2A-Hygro	PPI mapping
10	NL-TDP-43 3H10	donor cell line	AAVS1::T2A-Hygro	PPI mapping
11	mCit-TDP-43 2D11	acceptor cell line	AAVS1:: T2A-Neo	PPI mapping
12	mCit-TDP-43 4A7	acceptor cell line	AAVS1:: T2A-Neo	PPI mapping
	AAVS1:			
13	T2A-Hygro B6	donor recipient cell line	eHAP wild-type	N-terminal donor knock-in
14	T2A-Neo B6	acceptor recipient cell line	eHAP wild-type	N-terminal acceptor knock-in
15	T2A-Hygro-CAG-NL 1A3	donor control cell line	eHAP wild-type	donor control/bleed-through correction
16	T2A-Hygro-CAG-NL 1A4	donor control cell line	eHAP wild-type	donor control/bleed-through correction
17	T2A-Neo-CAG-mCit 1A4	acceptor control cell line	eHAP wild-type	acceptor control
18	T2A-Neo-CAG-mCit 1A5	acceptor control cell line	eHAP wild-type	acceptor control

Table 2: List of gRNAs sequences, genotyping and PCR primers.

#	Name	Sequence	Application
	ASPL:		
1	ASPSCR1_gDNA_fwd	GCTGGTGTCAGACAGGAAGCTG	genotyping
2	ASPSCR1_gDNA_rev	CACCTCACGTTCTCTCTCTTGTCAG	genotyping
3	ASPSCR1_gRNA	GTGCCCACTCCGCCAGCCAC	gRNA/knock-in
	UBXD1:		
4	UBXD1_gDNA_fwd	AGCGGCTGAGCGTGCTGC	genotyping
5	UBXD1_gDNA_rev	GTCCCTTCCTCCACCTTCACAGCCATG	genotyping
6	UBXD1_gRNA	GTTGTGAAATAAAAGCAGGGT	gRNA/knock-in
	VCP:		
7	VCP-N_gDNA_fwd	GACTTCTCTGGATTTGAGTG	genotyping
8	VCP-N_gDNA_rev	GTTAGTGCAACTCTAAACTGC	genotyping
9	VCP-C_gDNA_fwd	CTCTAGTAGTAGGATTGCAATC	genotyping
10	VCP-C_gDNA_rev	GTCCACATCAAATATAGGTG	genotyping
11	VCP-N_gRNA	ACGGCGCGCGCACACTCACT	gRNA/knock-in
12	VCP-C_gRNA	CAGGCCAGCTCACTGCACGC	gRNA/knock-in
	TDP-43:		
13	TARDBP_gDNA_fwd	CTTTAAGCAAGACACTTGATC	genotyping
14	TARDBP_gDNA_rev	ATATTAATCTATACCCACTGGC	genotyping
15	TARDBP-NT_gRNA	GAAAGATGTCTGAATATATTC	gRNA/knock-in
	AAVS1:		
16	A3-AAVS1_gDNA_fwd	CCCCCAGAATAGAATGACACC	genotyping
17	A2-AAVS1_gDNA_rev	CGGTTAATGTGGCTCTGGTT	genotyping
18	AAVS1_gRNA	GGGGCCACTAGGGACAGGAT	gRNA/knock-in
	HRT generation:		
19	AAVS1-Hyg-ins-SacI-SpeI-fw	GGCATCTTCCAGGGGTCCGAGAGCTCAGCTAGTCTTCTTC CTCCAACC	PCR & Gibson
20	AAVS1-Hyg-ins-SacI-SpeI-rev	CCCCGTAATTGATTACTATTAATAATCACAAATAAAGCATTT TTTTCACTGC	PCR & Gibson
21	P_AAVS1-Neo-only-fwd	P-GCCAGAGAGGATCCTGGG	PCR & ligation
22	P_AAVS1-Neo-only-rev	P-CCATAGAGCCCACCGCATC	PCR & ligation
23	P_AAVS1-Hygro-only-fwd	P-TAACTTGTTTATTGCAGCTTATAATGGTTAC	PCR & ligation
24	P_AAVS1-Hygro-only-rev	P-CTAGGGACAGGATTGGTGAC	PCR & ligation
25	Bb_TDP_NT_HDR-fwd	TACCTAATTTCAGCATTTTGATTAATTAACTGGCCTCATGGG CCTTC	PCR & Gibson
26	Bb_TDP_NT_HDR_rev	CCCGTGCCAGGACCTAACGATGGCGCGCCTAGGCCTTG	PCR & Gibson
27	HA-L_TDP_NT_HDR-fwd	GTCAAGGCCTAGGCGCGCCATCGTTAGGTCCTGGCACG	PCR & Gibson
28	HA-L_NL-TDP_NT-rev	AAATCTTCGAGTGTGAAGACCATCTTTTACTTTTCCTAAAGA GAAAAGAG	PCR & Gibson
29	HA-L_mCit-TDP_NT-rev	AGCTCTTCACCTTTCGATACCATCTTTTACTTTTCCTAAAGA GAAAAGAG	PCR & Gibson
30	HA-R_TDP_HDR-fwd	GCTCGGGAGGCTCGGGAGGCTCTGAATATATTCGGGTAAC CG	PCR & Gibson

31	HA-R_TDP_HDR-rev	CATGAGGCCAGTTAATTAATCAAAATGCTGAAATTAGGTATTTCC	PCR & Gibson
32	NL_ins_TDP_NT-HDR-fwd	TTTAGGAAAAGTAAAAGATGGTCTTCACACTCGAAGATTTCGTTGG	PCR & Gibson
33	NL_ins_TDP_NT-HDR-rev	GTTACCCGAATATATTCAGAGCCTCCCGAGCCTCCCGAGCCTCCCGAGCCTCCCGCCAGAATGCGTTCGC	PCR & Gibson
34	mCit_ins_TDP_NT_HDR-fwd	TTTAGGAAAAGTAAAAGATGGTATCGAAAGGTGAAGAGCTG	PCR & Gibson
35	mCit_ins_TDP_NT_HDR-rev	GTTACCCGAATATATTCAGAGCCTCCCGAGCCTCCCGAGCCTCCCGAGCCTCCACCAGCGGCTGTGAC	PCR & Gibson
36	UBXN6-HRT-5'-OH-FWD	AAGGAAGGCCGTCAAGGCCTAGGCGCGCCAATGGCTGCCTCCTGC	PCR & Gibson
37	UBXN6-HRT-5'-OH-REV	TCCCGAGCCTCCCGAGCCTCCCGAGCCTCCCAAGAGCTTCTCGATGGCTG	PCR & Gibson
38	UBXN6-HRT-3'-OH-FWD	ATAACTTCGTATAATGTATGCTATACGAAGTTATTGAAATAAAAGCAGGGTTGA	PCR & Gibson
39	UBXN6-HRT-3'-OH-REV	AAGGAAGGCCCATGAGGCCAGTTAATTAATCAGGTTCCAGGAATAGGATGT	PCR & Gibson
40	backbone-OH-UBXN6-FWD	GagacggccacatcctattcctggaacctgATTAATTAACTGGCCTCATGGGC	PCR & Gibson
41	backbone-OH-UBXN6-REV	GTTGGTGCCCACCCTGCAGGAGGCAGCCATTGGCGCGCCTAGGCC	PCR & Gibson
42	GSGS-NL-IRES2-Hygro-FWD	GAGCTCCTGTCAGCCATCGAGAAGCTCTTGGGAGGCTCGGGAGGC	PCR & Gibson
43	GSGS-NL-IRES2-Hygro-REV	ATAACTTCGTATAGCATACATTATACGAAGTTATCTATTCCTTTGCCCTCGGAC	PCR & Gibson
	Entry vectors:		
44	NanoLuc AttL1 fwd	GGGGACAAGTTTGTACAAAAAAGCAGGCTTCgccaccATGGTCTTCACACTCGAAG	PCR and BP
45	NanoLuc AttL2 rev	GGGGACCACTTTGTACAAGAAAGCTGGGTCCGCCAGAATGCGTTCGCAC	PCR and BP
46	attB1-mCit-fwd	GGGGACAAGTTTGTACAAAAAAGCAGGCTTCGCCACCATGGTATCGAAAGGTGAAGAGC	PCR and BP
47	attB2-mCit-rev	GGGGACCACTTTGTACAAGAAAGCTGGGTCTCAACCAGCGGCTGTGAC	PCR and BP

Figure 1

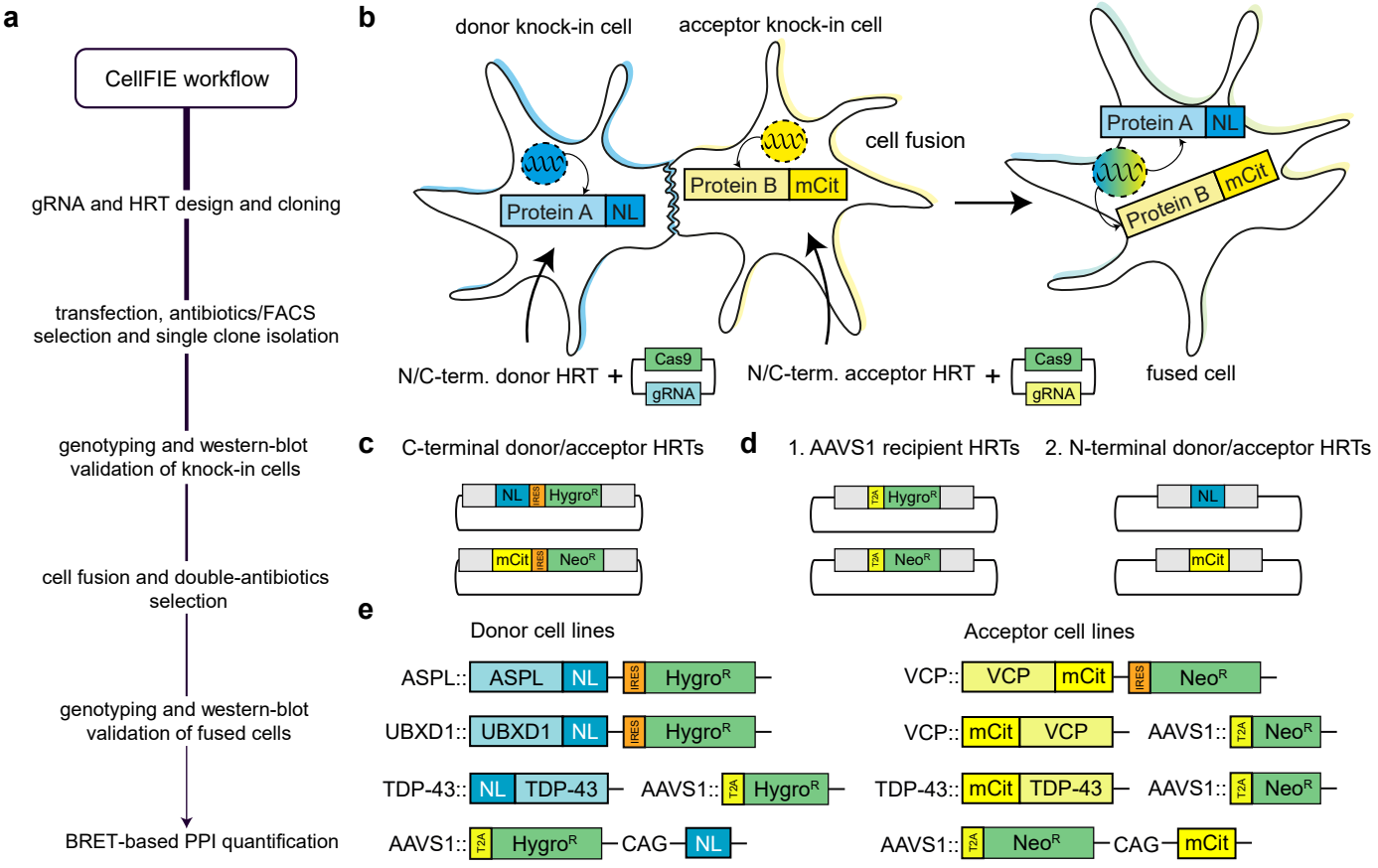
a
CellFIE workflow
gRNA and HRT design and cloning
transfection, antibiotics/FACS selection and single clone isolation
genotyping and western-blot validation of knock-in cells
cell fusion and double-antibiotics selection
genotyping and western-blot validation of fused cells
BRET-based PPI quantification
b
donor knock-in cell
acceptor knock-in cell
cell fusion
Protein A
NL
Protein B
mCit
N/C-term. donor HRT
Cas9
gRNA
N/C-term. acceptor HRT
fused cell
c
C-terminal donor/acceptor HRTs
IRES
Hygro^R
Neo^R
d
1. AAVS1 recipient HRTs
2. N-terminal donor/acceptor HRTs
T2A
e
Donor cell lines
Acceptor cell lines
ASPL::
UBXD1::
TDP-43::
AAVS1::
CAG
VCP::

Figure 2

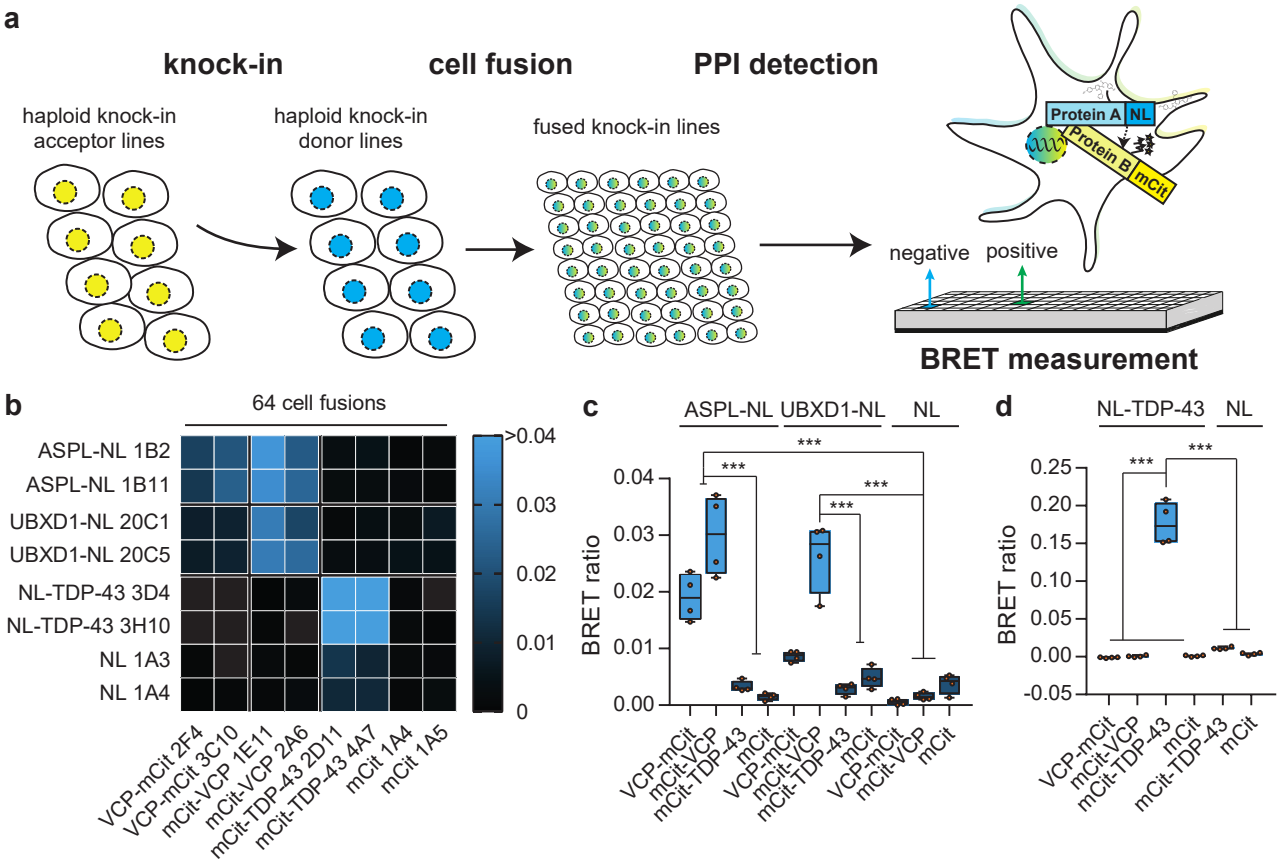
a
knock-in
cell fusion
PPI detection
haploid knock-in acceptor lines
haploid knock-in donor lines
fused knock-in lines
Protein A
NL
Protein B
mCit
negative
positive
BRET measurement
b
64 cell fusions
ASPL-NL 1B2
ASPL-NL 1B11
UBXD1-NL 20C1
UBXD1-NL 20C5
NL-TDP-43 3D4
NL-TDP-43 3H10
NL 1A3
NL 1A4
>0.04
0.03
0.02
0.01
0
VCP-mCit 2F4
VCP-mCit 3C10
mCit-VCP 1E11
mCit-VCP 2A6
mCit-TDP-43 2D11
mCit-TDP-43 4A7
mCit 1A4
mCit 1A5
c
ASPL-NL
UBXD1-NL
NL
BRET ratio
0.04
0.03
0.02
0.01
0.00
***
VCP-mCit
mCit-VCP
mCit-TDP-43
mCit
d
NL-TDP-43
NL
BRET ratio
0.25
0.20
0.15
0.10
0.05
0.00
-0.05

Figure 3

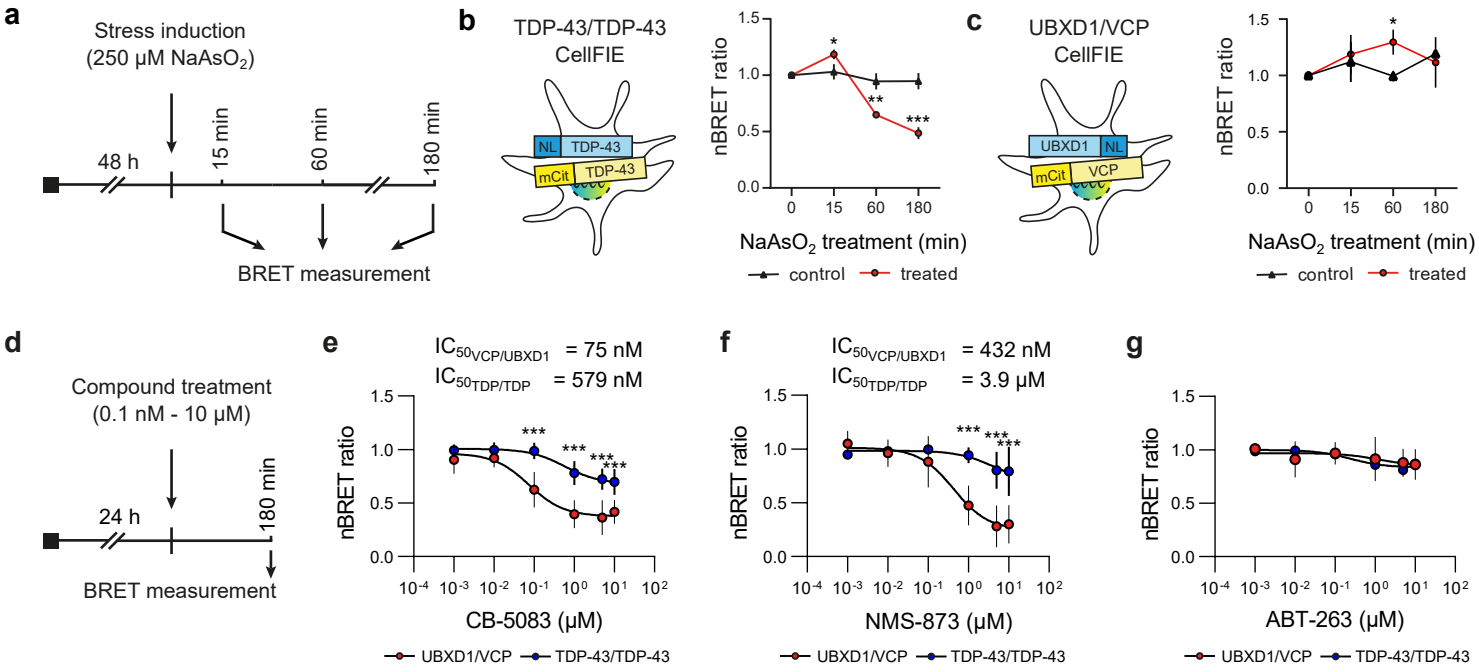
a
Stress induction
(250 µM NaAsO2)
48 h
15 min
60 min
180 min
BRET measurement
b
TDP-43/TDP-43
CellFIE
NL
TDP-43
mCit
TDP-43
nBRET ratio
NaAsO2 treatment (min)
control
treated
c
UBXD1/VCP
CellFIE
UBXD1
NL
mCit
VCP
nBRET ratio
NaAsO2 treatment (min)
control
treated

d
Compound treatment
(0.1 nM - 10 µM)
24 h
180 min
BRET measurement
e
IC50VCP/UBXD1 = 75 nM
IC50TDP/TDP = 579 nM
nBRET ratio
CB-5083 (µM)
UBXD1/VCP
TDP-43/TDP-43
f
IC50VCP/UBXD1 = 432 nM
IC50TDP/TDP = 3.9 µM
nBRET ratio
NMS-873 (µM)
UBXD1/VCP
TDP-43/TDP-43
g
nBRET ratio
ABT-263 (µM)
UBXD1/VCP
TDP-43/TDP-43

Supplementary Fig. 1

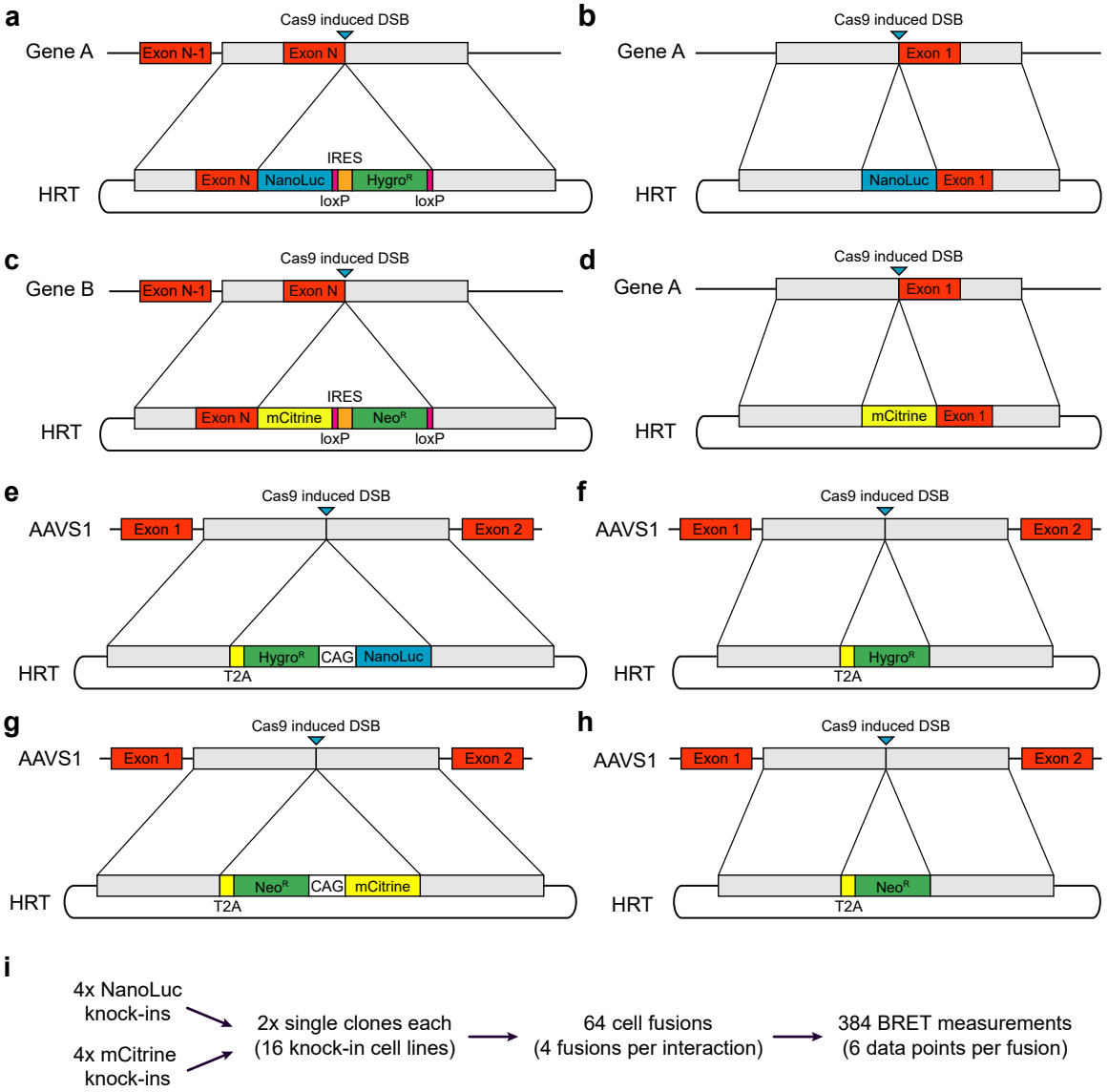

Supplementary Fig. 2

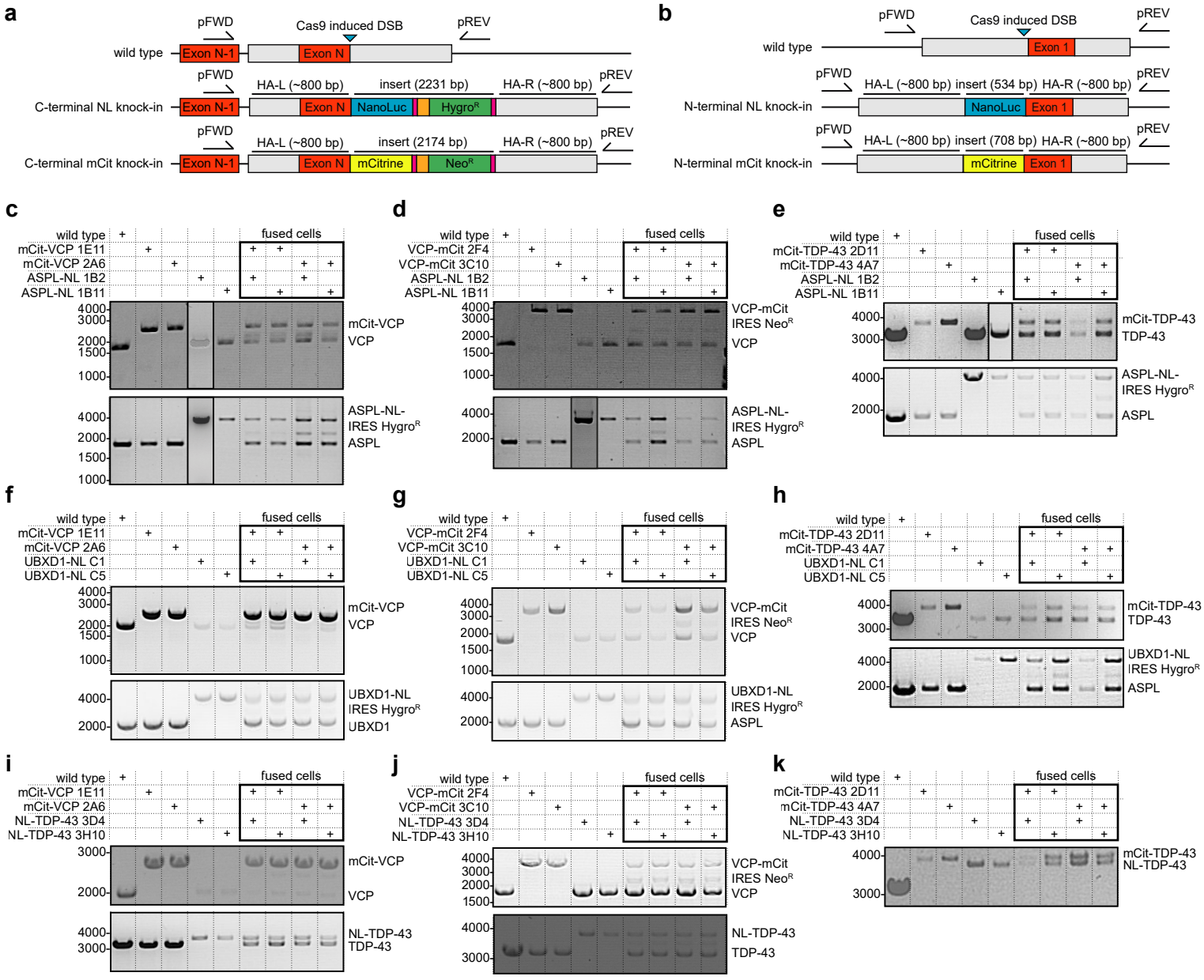

Supplementary Fig. 3